SLAC-PUB-13562

Dark Matter in the MSSM

R C Cotta, J S Gainer, J L Hewett and T G Rizzo

SLAC National Accelerator Laboratory, 2575 Sand Hill Rd., Menlo Park, CA, 94025, USA

E-mail: rcotta@stanford.edu, jgainer@slac.stanford.edu, hewett@slac.stanford.edu, rizzo@slac.stanford.edu

Abstract. We have recently examined a large number of points in the parameter space of the phenomenological MSSM, the 19-dimensional parameter space of the CP-conserving MSSM with Minimal Flavor Violation. We determined whether each of these points satisfied existing experimental and theoretical constraints. This analysis provides insight into general features of the MSSM without reference to a particular SUSY breaking scenario or any other assumptions at the GUT scale. This study opens up new possibilities for SUSY phenomenology at colliders as well as in both direct and indirect detection searches for dark matter.

Submitted to: *New J. Phys.*

1. Introduction

Supersymmetry (SUSY) represents an appealing possibility for Beyond the Standard Model Physics; its discovery would help provide answers to many of the preeminent questions in particle physics, astrophysics, and cosmology. However, as no sparticles have been observed, it is clear that if SUSY exists, it must be broken. The mechanism which could break SUSY is a question of great importance, and there is an ever growing list of possible scenarios, including mSUGRA[1], GMSB[2], AMSB[3], and gaugino mediated supersymmetry breaking[4]. In each of these scenarios, the SUSY spectrum is described by a handful of parameters, generally defined at the SUSY breaking scale; straightforward RGE running of sparticle masses and coupling constants yields predictions for the mass spectra and decay patterns of the various sparticles at energy scales relevant for colliders or cosmology. However, these SUSY breaking scenarios are restrictive and predict specific phenomenologies for colliders and cosmology that do not represent the full range of possible SUSY signatures.

It is clearly desirable to study the MSSM more broadly without making simplifying assumptions at the high scale that may turn out to be unwarranted. However, the MSSM requires 105 parameters to describe SUSY breaking, in addition to the parameters of the SM[5]. Obviously this is far too many parameters to study directly, so some simplifying assumptions must be made. Here we will restrict ourselves to the CP-conserving MSSM (*i.e.*, no new phases) with minimal flavor violation (MFV)[6]. Additionally, we require that the first two generations of sfermions be degenerate as motivated by constraints from flavor physics. We are then left with 19 independent, real, weak-scale, SUSY Lagrangian parameters, namely the gaugino masses $M_{1,2,3}$, the Higgsino mixing parameter μ, the ratio of the Higgs vevs $\tan\beta$, the mass of the pseudoscalar Higgs boson m_A, and the 10 squared masses of the sfermions ($m_{\tilde{q}1,3}$, $m_{\tilde{u}1,3}$,$m_{\tilde{d}1,3}$,$m_{\tilde{l}1,3}$,and $m_{\tilde{e}1,3}$). We include independent A-terms only for the third generation (A_b, A_t, and A_τ) due to the small Yukawa couplings for the first two generations. This set of 19 parameters has been called the phenomenological MSSM (pMSSM)[7].

To study the pMSSM, we performed a scan over this 19-dimensional parameter space assuming flat priors for the specified ranges[8]:

$$\begin{aligned}
&100\,\mathrm{GeV} \leq m_{\tilde{f}} \leq 1\,\mathrm{TeV}\,,\\
&50\,\mathrm{GeV} \leq |M_{1,2},\mu| \leq 1\,\mathrm{TeV}\,,\\
&100\,\mathrm{GeV} \leq M_3 \leq 1\,\mathrm{TeV}\,,\\
&|A_{b,t,\tau}| \leq 1\,\mathrm{TeV}\,,\\
&1 \leq \tan\beta \leq 50\,,\\
&43.5\,\mathrm{GeV} \leq m_A \leq 1\,\mathrm{TeV}\,.
\end{aligned} \tag{1}$$

The value of 43.5 GeV in the last constraint was chosen to avoid the possible on-shell decay $Z \to hA$. We randomly generated 10^7 points in this parameter space and subjected them to a number of existing theoretical and experimental constraints. We also performed a scan with log priors and slightly different mass ranges (that we will

not employ here) in order to gauge the influence of priors on our results; we found that these results are substantially similar to those obtained in our flat prior scan[8]. Using these parameters we generate a SUSY spectrum utilizing SuSpect2.34[7]. By convention, the parameters are specified at the scale given by the geometric mean of the two stop masses. The input values for the SM parameters used in our analysis are given in [8].

We then apply a series of constraints obtaining a set of models that satisfy all existing theoretical and experimental data. (This is the so-called "flat prior" set obtained in Ref.[8].) In the analysis below we will discuss the applied constraints then will examine the properties of the LSP at the parameter points which remain viable. In particular, we will examine the gaugino and Higgsino content of the LSP (which is always the lightest neutralino). We will also discuss the nature of the nLSP and the difference between its mass and the LSP mass; this is important, for example, in coannihilation processes. We will then examine the signatures in direct and indirect WIMP detection experiments obtained for these points in parameter space.

2. Theoretical and Experimental Constraints

We now discuss the theoretical and experimental constraints which we applied to the generated parameter space points (which we shall hereafter refer to as "models" for convenience). We will present each of these briefly in turn; for more details, one should consult [8].

2.1. Theoretical Constraints

We demand that the sparticle spectrum not have tachyons or color or charge breaking (CCB) minima in the scalar potential. We also require that the Higgs potential be bounded from below and that electroweak symmetry breaking be consistent. We assume that the LSP, which will be absolutely stable, be a conventional thermal relic so that the LSP can be identified as the lightest neutralino. If it is a significant component of the dark matter, the LSP must be uncolored and uncharged, thus the LSP can only be a sneutrino or a neutralino. The possibility that the LSP is a sneutrino can be easily eliminated in the pMSSM by combining several of the experimental constraints, particularly those involving direct detection of sneutrino WIMPs and the invisible width of the Z, as discussed below.

2.2. Low Energy Constraints

The code micrOMEGAs2.20[9] was used to evaluate the following observables for each point in the parameter space: $\Delta\rho$, the decay rates for $b \to s\gamma$ and $B_s \to \mu^+\mu^-$, and the $g-2$ of the muon. In addition, we evaluate the branching fraction for $B \to \tau\nu$ following[10] and [11]. The ranges that we allow for these observables are listed in Table 1. The large range for the SUSY contribution to $g-2$ ($\sim 6\sigma$) is due to the evolving discrepancy between theory and experiment[12].

Constraint	Range	References
$\Delta\rho$	-0.0007 - 0.0026	[14]
$b \to s\gamma$	2.5×10^{-4} - 4.1×10^{-4}	[15][16][17]
$B_s \to \mu^+\mu^-$	0 - 4.5×10^{-8}	[18]
$\Delta_{\rm SUSY}(g-2)_\mu$	-1.0×10^{-9} - 4.0×10^{-9}	[12][19][20]
$B \to \tau\nu$	5.5×10^{-5} - 2.27×10^{-4}	[10][11][15][21]

Table 1. Ranges allowed for various low energy observables in our analysis.

We implemented constraints from meson-antimeson mixing[13] by assuming MFV[6], imposing first and second generation mass degeneracy, and demanding that the ratio of first/second and third generation squark soft breaking masses (of a given flavor and helicity) differ from unity by no more than a factor of 5. We also imposed analogous restrictions in the slepton sector.

2.3. LEP Constraints

We now consider the constraints that arise from LEP data. Due to running LEP at the Z pole, it is very unlikely that there can be charged sparticles with masses below $M_Z/2$. The same constraint is applied to the lightest neutral Higgs boson. Data from LEPII[22] suggests that there are no new *stable* charged particles of any kind with masses below 100 GeV. We also require that any new contributions to the invisible width of the Z boson be ≤ 2 MeV[23]; this constraint eliminates the possibility of certain species of neutralinos having masses below $M_Z/2$.

Following ALEPH[24] we implement a lower limit of 92 GeV on first and second generation squark masses, provided that the gluino is more massive than the squarks and the mass difference (Δm) between the squark and the LSP is ≥ 10 GeV. We also implement a similar cut (following [25]) on the mass of sbottom quarks requiring that their mass be greater than 95 GeV (in addition to $\Delta m \geq 10$ GeV, and the mass being less than the gluino mass). The situation for stops is slightly more complex[26]; we demand that the lightest stop mass be greater than 97 GeV if the stop is too light to decay into $Wb\chi_1^0$. If the stop can decay to $\ell b\tilde{\nu}$; we have a lower limit of 95 GeV on its mass.

Following [26], we demand that right-handed sleptons have masses greater than 100, 95, or 90 GeV for selectrons, smuons, and staus respectively. We only apply this limit when the condition $0.97m_{\rm slepton} > m_{\rm LSP}$ is satisfied. We can also apply these bounds to left-handed sleptons, provided that the neutralino $t-$channel diagram may be neglected in the case of selectrons; we assume that this is the case.

We demand that chargino masses be greater than 103 GeV, provided that the LSP-chargino mass splitting is $\Delta m > 2$ GeV[26]. If $\Delta m < 2$ GeV, the bound is 95 GeV. It should be noted that when Δm is very small ($\lesssim 100\,{\rm MeV}$), the chargino is stable for detector length scales and the model will be excluded by the stable charged particle

constraints. In the case where the lightest chargino is dominantly Wino, we can only apply this limit when the electron sneutrino $t-$channel diagram is negligible; we take this to be the case when the electron sneutrino is more massive than 160 GeV.

The LEP Higgs Working Group[27], provides five sets of constraints on the MSSM Higgs sector imposed by LEPII data. These are essentially limits on the Higgs-Z coupling times the branching fraction for decay to given final states, as a function of the Higgs masses. We employ SUSY-HIT[28] to analyze these. We include a theoretical uncertainty on the calculated mass of the lightest Higgs boson of approximately 3 GeV[29] when applying these constraints.

2.4. Tevatron Constraints

We also employ constraints from the Tevatron. We obtained restrictions on the squark and gluino sectors arising from the null result of the D0 multijet plus missing energy search[30]. We generalize their analysis to render it model independent, by generating multijet plus missing energy events for our model spectrum using PYTHIA6.4[31] (which we provide with a SUSY-HIT[28] decay table) as interfaced to PGS4 [32]. PGS4 provides a fast detector simulation and is used to impose the kinematic cuts used in the D0 analysis. We weigh our results with K factors computed using PROSPINO2.0 [33]. The 95% CL upper limit on the number of signal events, as defined by the D0 analysis, is 8.34 (for the 2.1 fb^{-1} data set considered) using the method of Feldman and Cousins[34]. Analogously, we employ constraints from the CDF search for trileptons plus missing energy[35], which we also generalize to the full pMSSM. We only make use of the CDF '3 tight lepton' analysis as it is the cleanest and easiest to implement with PGS4; we also use a K-factor of 1.3 for all models. Here the 95% CL upper bound on the possible SUSY signal in the channel we are considering is 4.65 events for the luminosity of 2.02 fb^{-1} used in the CDF analysis.

In addition to these collider signature bounds, we also employ the experimental constraint[36] resulting from direct searches for the new Higgs fields in the MSSM: for the narrow mass range $90 \leq m_A \leq 100$, $\tan\beta$ is restricted to the region $\tan\beta \geq 1.2m_A - 70$. This range is excluded as the Tevatron would have otherwise discovered at least one of the heavier Higgs bosons. Also, D0[37] has obtained lower limits on the mass of heavy stable charged particles. We take this constraint to be $m_{\chi^+} \geq 206|U_{1w}|^2 + 171|U_{1h}|^2$ GeV at 95% CL for charginos, where the matrix entries U_{1w} and U_{1h} determine the Wino/Higgsino content of the lightest chargino. We use this to interpolate between the separate Wino and Higgsino results provided by D0.

CDF and D0 also have analyses that search for light stops and sbottoms[38] which include a number of assumptions about the SUSY mass spectrum, sparticle decay channels, etc. In general they are only applicable when the sbottoms or stops are lighter than the top quark. These searches are difficult to implement in a model-independent pMSSM context. Thus we exclude models with light ($m < m_t$) stops or sbottoms from our final set of models; this only affected ~ 1000 models.

2.5. Astrophysical Constraints

There are two constraints from considering the LSP as a long-lived relic. As noted above, we demand that the LSP be the lightest neutralino. We also require, following the 5 year WMAP measurement[39] of the relic density, that $\Omega h^2|_{\rm LSP} \leq 0.121$. In not employing a lower bound on $\Omega h^2|_{\rm LSP}$ for our models, we acknowledge the possibility that even within the MSSM and the thermal relic framework, dark matter may have multiple components with the LSP being just one possible contributor; we thus only require that the LSP not have a relic density too large to be consistent with WMAP. However, in discussing results below, we will also discuss a subset of models for which $0.1 \leq \Omega h^2|_{LSP} \leq 0.121$; these represent the more standard assumption that the LSP is the dominant, perhaps only, component of the relic density.

We also obtain constraints from attempts to detect dark matter directly[40]. Generally, the strongest constraints come from the spin-independent WIMP-nucleon cross sections, hence we only implement bounds on our models from these; inspection of the spin-dependent WIMP-nucleon cross sections in our models confirms that this approach is reasonable. Both spin-independent and spin-dependent cross sections were calculated using micrOMEGAs2.21[9]. We implement cross section limits from XENON10[41], CDMS[42], CRESST I[43] and DAMA[44] data. Since these cross sections depend on some low energy quantities for which the uncertainties are relatively large (*e.g.*, nuclear form factors), we do not exclude models with WIMP-nucleon spin-independent cross sections as much as 4 times larger than the experimental bounds. It should be noted that many of our models predict a value $\Omega h^2|_{\rm LSP}$ which is less than that observed by WMAP and supernova searches. We thus scale our cross sections to take this into account.

3. Results

As noted above we randomly generated 10^7 parameter space points (*i.e.*, models) in a 19-dimensional pMSSM parameter space using flat priors. Only $\sim 68.5 \cdot 10^3$ of these models satisfy all the constraints listed in the previous section. The properties of these models are described in much greater detail in [8]. Here we will discuss the attributes of these models which are most important astrophysically. In particular we will examine the mass and composition of the LSP and nLSPs, the predicted relic density, as well as direct and indirect dark matter detection signals from these models.

3.1. LSP and nLSP

Figure 1 presents a histogram of the masses of the four neutralino species in our models; Figure 2 displays a similar histogram for the two chargino species. The lightest neutralino is, of course, the LSP. The LSP mass lies between 100 and 250 GeV in over 70% of our models. Generally models with a mostly Higgsino or Wino LSP have a chargino with nearly the same mass as the LSP; as sufficiently light charginos would

normally have been detected at LEP or the Tevatron, there are fewer models with such LSPs with mass $\lesssim$ 100 GeV.

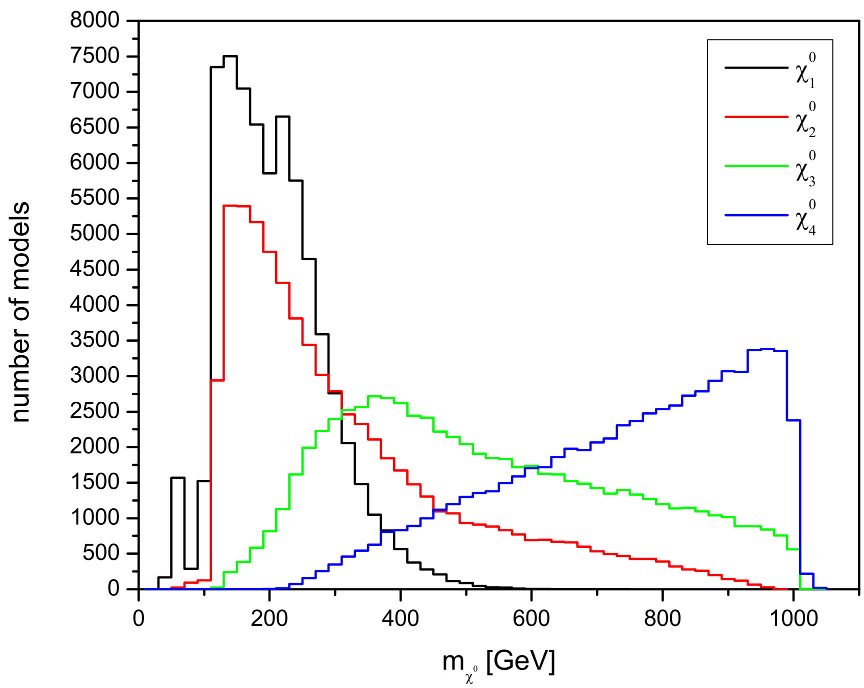

Figure 1. Distribution of neutralino masses for our set of models.

The identity of the nLSP is shown in Figure 3. The lightest chargino is the nLSP in about 78% of the models; this is due to many models having Wino or Higgsino LSPs, and the generally small mass splitting between a mostly Wino or Higgsino neutralino and the corresponding chargino. The second lightest neutralino is the nLSP $\sim 6\%$ of the time. These will generally be models with a dominantly Higgsino LSP. Note also that while neutralinos or charginos are the nLSP in the vast majority of cases, there are 10 other sparticles each of which is the nLSP in $> 1\%$ of our models. Scenarios in which these sparticles are the nLSP may lead to interesting signatures at the LHC[45].

Figure 4 displays the LSP mass value as a function of the LSP-nLSP mass splitting, Δm, our models for each identity of the LSP. It is interesting that these models have a smaller Δm than is often considered; 80% of our models have $\Delta m < 10$ GeV, 27% have $\Delta m < 1$ GeV, and 3% have $\Delta m < 10$ MeV. As one can see from Figure 4, this occurs largely, but not exclusively, in models with a chargino nLSP. This is again due to the many models where the LSP is nearly pure Wino or Higgsino.

There are a number of interesting features in this figure. The mostly empty square region which appears on the lower left-hand side of Figure 4 is due to the fact that models with chargino nLSPs in this mass and Δm range have been excluded by the

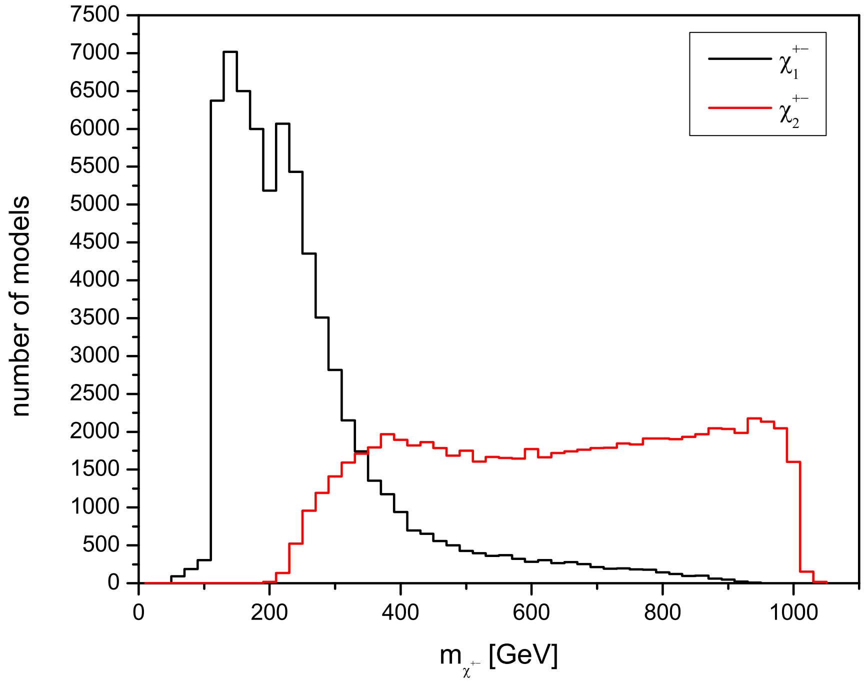

Figure 2. Distribution of chargino masses for our set of models.

Tevatron stable chargino search. Non-chargino nLSPs are not eliminated by this search (*e.g.*, the production cross section for sleptons in this range is too small to be excluded by the Tevatron search). It is perhaps worth noting that a stable heavy charged particle search at the LHC, corresponding to those done at the Tevatron, would be able to exclude or discover the models with heavier chargino nLSPs and small values of Δm (corresponding to $\sim 12\%$ of our model set).

Another interesting feature in this figure is the bulge for 0.1 GeV $\leq \Delta m \lesssim$ 2 GeV and $m_{LSP} \lesssim$ 100 GeV. This region exists because these values of Δm are large enough that at LEP or the Tevatron, the produced chargino would decay in the detector, but the resulting charged tracks would be too soft to be observed. The existence of such a region shows the difficulty of making model independent statements about sparticle masses or other SUSY observables.

We have seen that within our model set the nLSP can be almost any SUSY particle and the corresponding Δm can be small for these cases. Thus specific models in our set describe qualitatively most of the conventional long-lived sparticle scenarios. Long-lived stops or staus (as in GMSB[2]), gluinos (as in Split SUSY[46]) as well as charginos (as in AMSB[3]) all occur in our sample. We also have long-lived neutralinos, as does GMSB, however these are the $\tilde{\chi}_2^0$ in our case. In addition to models which, to some extent, correspond to these well-studied scenarios, we also have models with long-lived

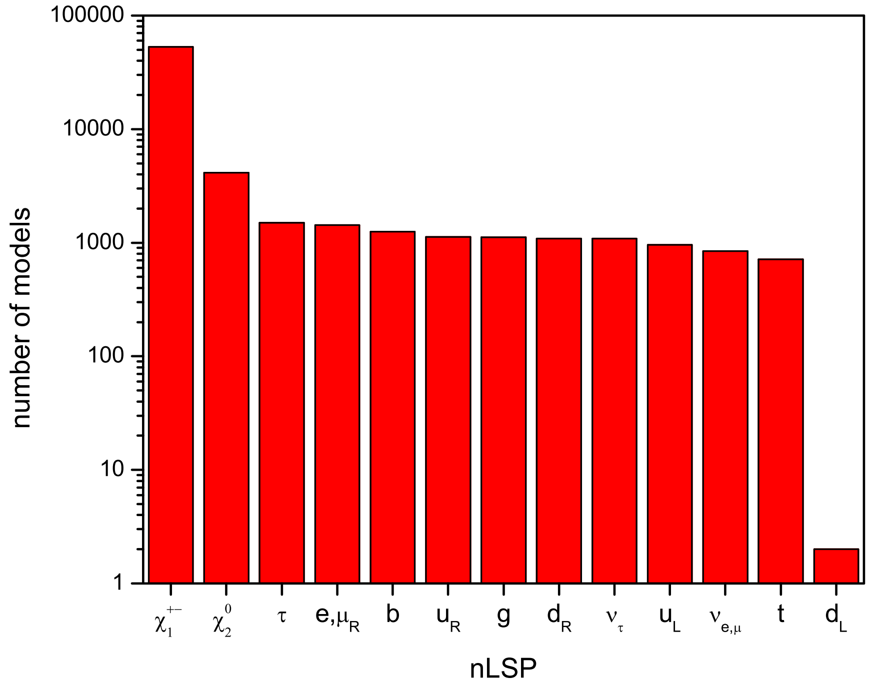

Figure 3. Number of models in which the nLSP is the given sparticle.

selectrons, sneutrinos and sbottoms.

Figures 5, 6, and 7 display the gauge eigenstate content of the LSPs in our model set. We note that most LSPs are relatively pure eigenstates, with models where the LSP is Higgsino or mostly Higgsino being by far the most common. About one quarter of our models have Wino or mostly Wino LSPs, while just over one-sixth have Bino or mostly Bino LSPs. Within mSUGRA, the LSP is, in general, nearly purely Bino; this suggests that most of our models are substantially different from mSUGRA. A more precise breakdown of the content of LSPs in the model set is presented in Table 2. We note that one would expect the LSP be a pure eigenstate fairly often in a random scan of Lagrangian parameters, since if the differences between M_1, M_2, and μ are large compared to M_Z, then the eigenstates of the mixing matrix will be essentially pure gaugino and Higgsino states[5].

3.2. Relic Density

We did not demand that the LSP, in any given model, account for all of the dark matter, rather we required only that the LSP relic density not be too large to be consistent with WMAP. More specifically, we employed $\Omega h^2|_{\rm LSP} < 0.121$. Figure 8 shows the distribution of $\Omega h^2|_{\rm LSP}$ values predicted by our model set. Note that this distribution is peaked at small values of $\Omega h^2|_{\rm LSP}$. In particular, the mean value for this quantity in

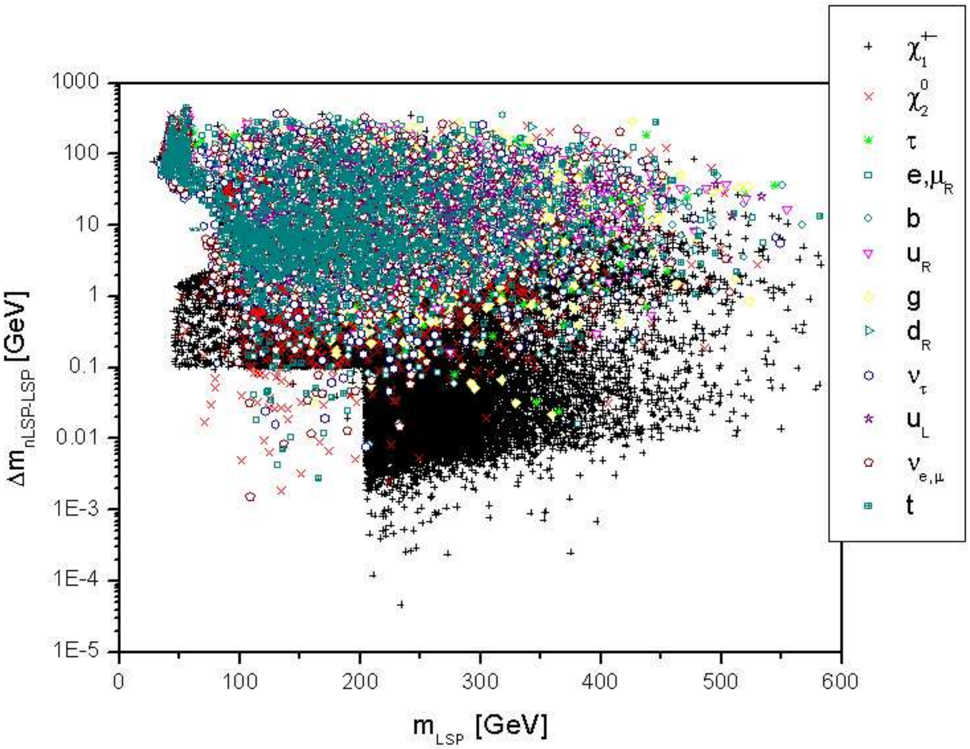

Figure 4. Mass splitting between nLSP and LSP versus LSP mass. The identity of the nLSP is shown as well. (The LSP is always the lightest neutralino in our set of models).

LSP Type	Definition	Fraction of Models
Bino	$\|Z_{11}\|^2 > 0.95$	0.14
Mostly Bino	$0.8 < \|Z_{11}\|^2 \leq 0.95$	0.03
Wino	$\|Z_{12}\|^2 > 0.95$	0.14
Mostly Wino	$0.8 < \|Z_{12}\|^2 \leq 0.95$	0.09
Higgsino	$\|Z_{13}\|^2 + \|Z_{14}\|^2 > 0.95$	0.32
Mostly Higgsino	$0.8 < \|Z_{13}\|^2 + \|Z_{14}\|^2 \leq 0.95$	0.12
All other models		0.15

Table 2. The fractions of our model set for which the LSP is of each of the given types. These types are defined here by the modulus squared of elements of neutralino mixing matrix in the SLHA convention. See [5] for details.

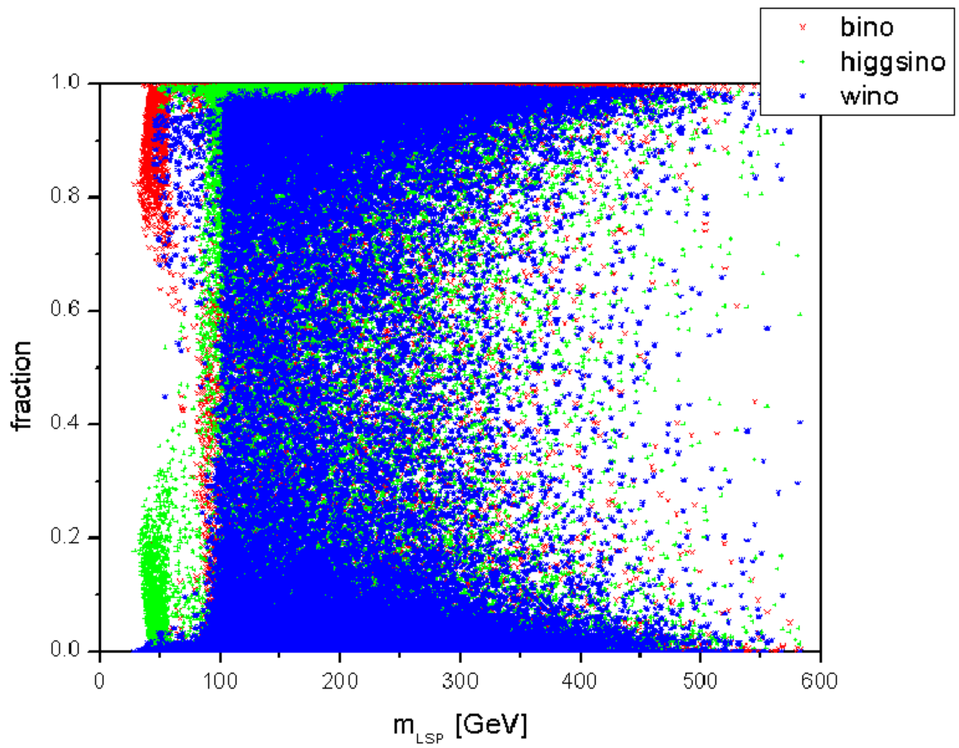

Figure 5. The distribution of LSP gaugino eigenstate types as a function of the LSP mass. Note that each LSP corresponds to three points on this figure, one each for its Bino, Wino, and Higgsino fraction.

our models is ~ 0.012, which is about ten times less than the central value determined from the aforementioned WMAP and supernova data[39]. We note that the range of possible values of $\Omega h^2|_{\mathrm{LSP}}$ is found to be much larger than those obtained by analyses of specific SUSY breaking scenarios[47].

We display the predictions for $\Omega h^2|_{\mathrm{LSP}}$ versus the LSP mass in Figure 9 and versus the nLSP - LSP mass splitting in Figure 10. Figure 9 makes it clear that $\Omega h^2|_{\mathrm{LSP}}$ generally increases with the LSP mass, but a large range of values for the relic density are possible at any given LSP mass. The empty region in Figure 9 where $\Omega h^2|_{\mathrm{LSP}} \approx 0.001 - 0.1$ and $m_{\mathrm{LSP}} \approx 50 - 100$ is due to the fact that, in general, LSPs which are mostly Higgsino or Wino give lower values of $\Omega h^2|_{\mathrm{LSP}}$, and, as noted above, there are fewer Higgsino or Wino LSPs in this mass range. Figure 10 shows that small mass differences can lead to large dark matter annihilation rates.

3.3. Direct Detection of Dark Matter

As noted above, we calculate the spin-dependent and spin-independent WIMP-nucleon cross sections using micrOMEGAs 2.21 [9]. These data give the possible signatures in our model set for experiments that search for WIMPs directly. As these experiments

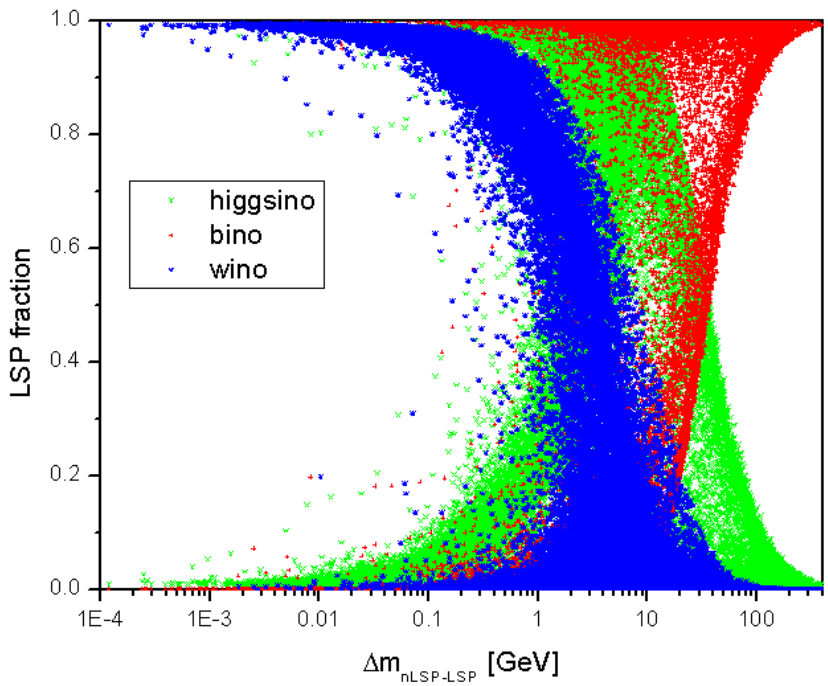

Figure 6. The distribution of LSP gaugino eigenstate types as a function of the LSP-nLSP mass difference. Note that as in Figure 5, every LSP corresponds to three points on this figure, one each for its Bino, Wino, and Higgsino fractions.

measure the product of WIMP-nucleon cross sections with the local relic density, the cross section data presented in the figures below are scaled by $\xi = \Omega h^2|_{\rm LSP}/\Omega h^2|_{\rm WMAP}$. To date, these experiments generally provide a more significant bound on the spin-independent cross section, and hence we will focus on those.

Figure 11 presents the distribution for the scaled WIMP-proton spin-independent cross section versus relic density for our model sample. As one would expect, larger values of the cross section are generally found at larger values of $\Omega h^2|_{\rm LSP}$. However, even for relic densities close to the WMAP value, $\xi\sigma_{p,SI}$ is seen to vary by almost eight orders of magnitude. These ranges for $\xi\sigma_{p,SI}$ are much larger than those from mSUGRA as calculated, *e.g.*, in [48].

Figure 12 shows the scaled WIMP-proton spin-dependent and spin-independent cross sections as a function of the LSP mass. The constraints from XENON10[41] and CDMS[42] are also displayed. As noted above, to take the uncertainties in the theoretical calculations of the WIMP-nucleon cross section into account, we allowed for a factor of 4 uncertainty in the calculation of the WIMP-nucleon cross section. Table 3 gives the fraction of models that would be excluded if the combined CDMS/XENON10 cross section limit were improved by an overall scaling factor. Note that our inclusion of the theoretical uncertainties does not significantly modify the size of our model sample.

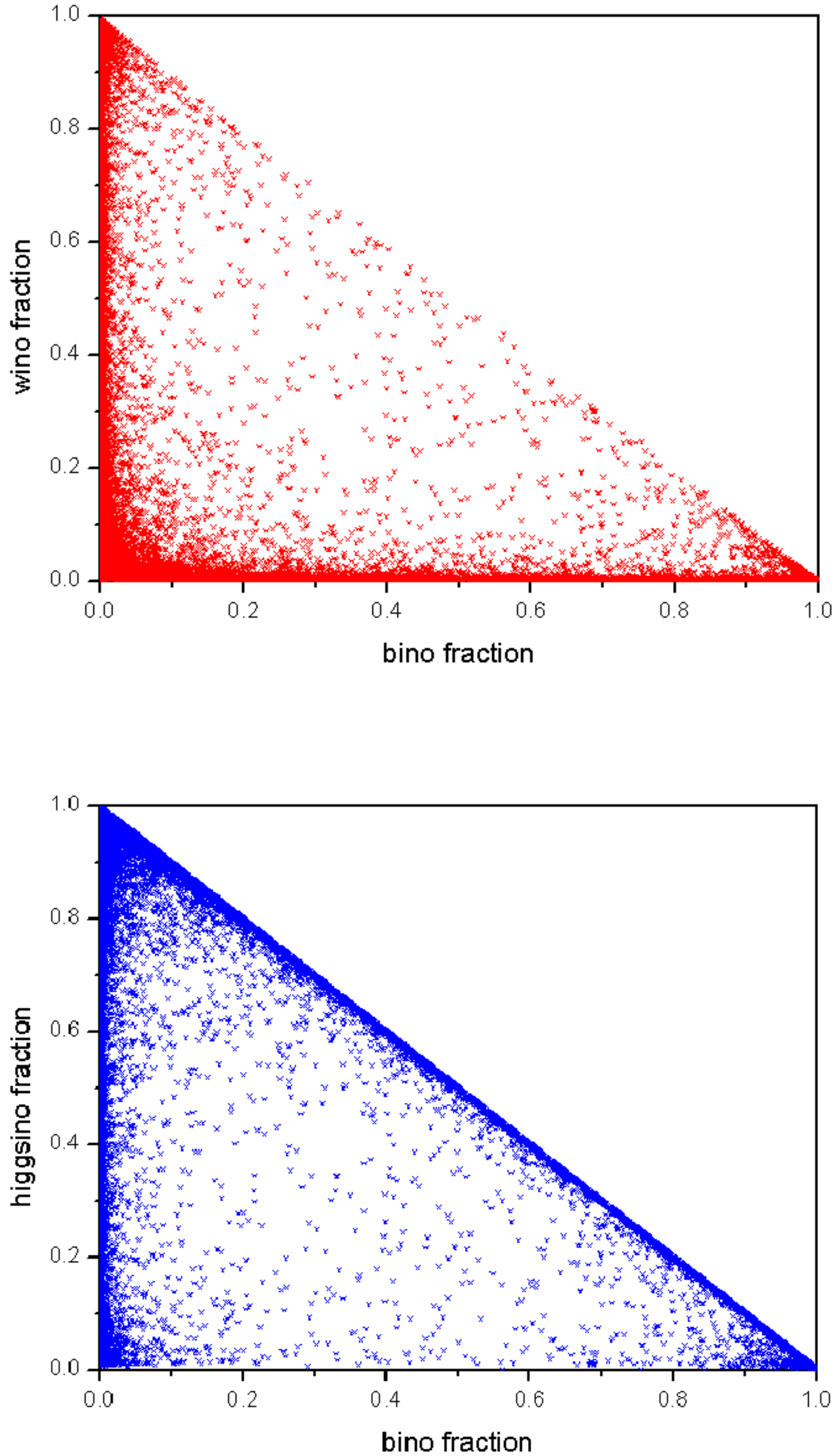

Figure 7. Wino/Higgsino/Bino content of the LSP in the case of flat priors. Note that, as elsewhere in the paper, $|Z_{11}|^2$, $|Z_{12}|^2$, and $|Z_{13}|^2+|Z_{14}|^2$, where Z_{ij} is the neutralino mixing matrix in the SLHA convention[5], give the Bino, Wino, and Higgsino fractions respectively.

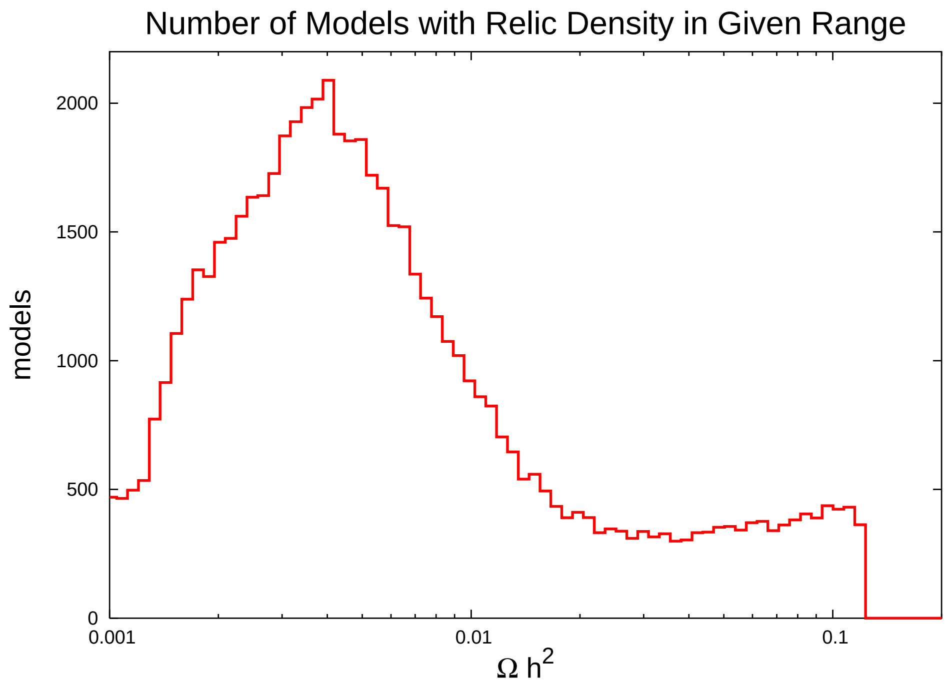

Figure 8. Distribution of $\Omega h^2|_{\rm LSP}$ for our models.

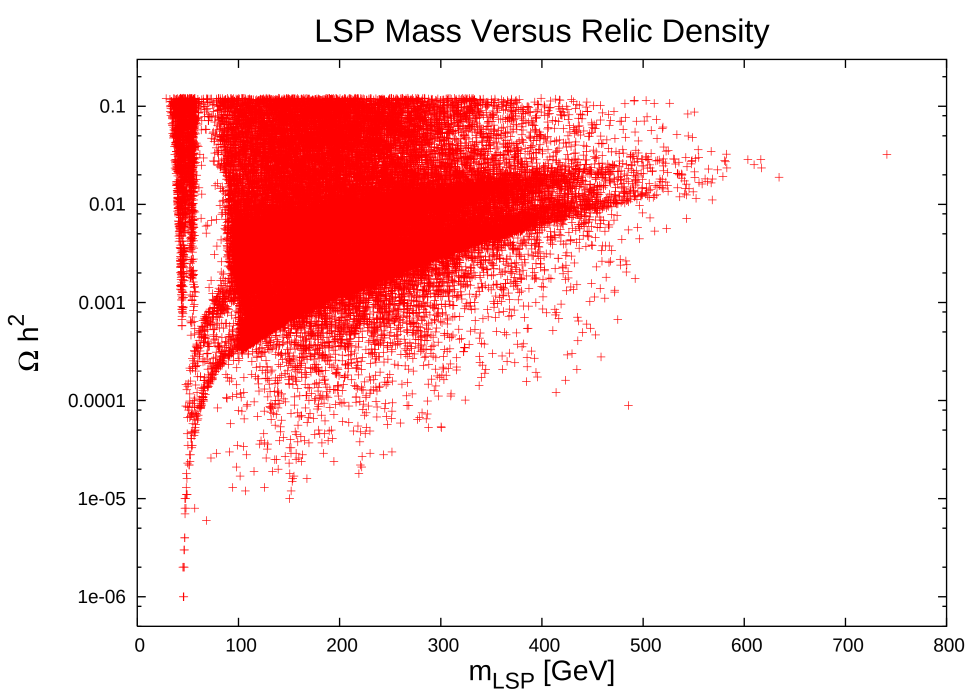

Figure 9. Distribution of $\Omega h^2|_{\rm LSP}$ as a function of the LSP mass.

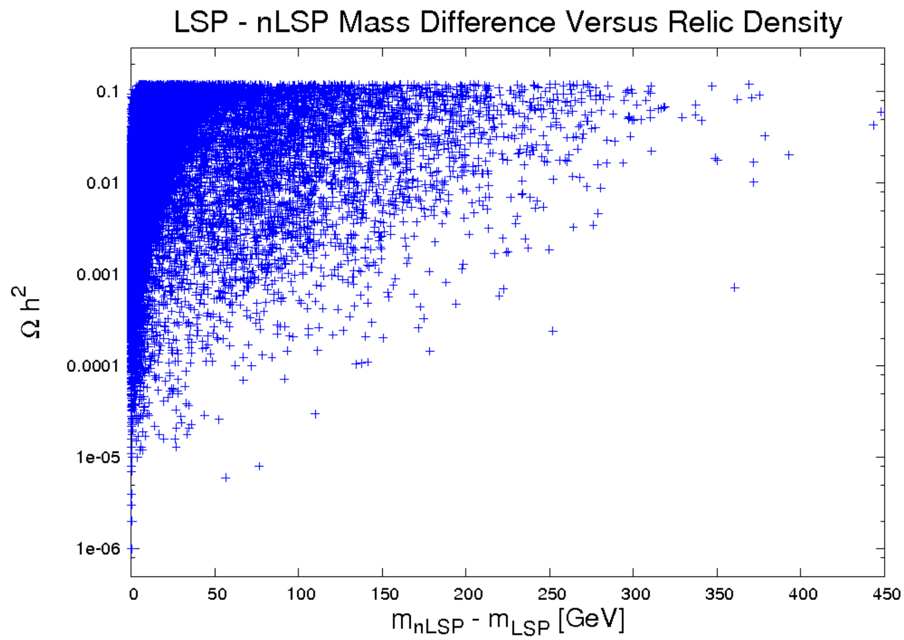

Figure 10. Distribution of $\Omega h^2|_{\rm LSP}$ as a function of the LSP-nLSP mass splitting.

Improvement in S.I. Cross Section Limit	Fraction of Models Excluded
4	0.032
10	0.071
40	0.19
100	0.31
400	0.52
1000	0.65
4000	0.81

Table 3. The fraction of our model set which would be excluded for the specified improvement in the direct detection bound on the spin-independent WIMP-nucleon cross section.

We find that the range of values obtained for these cross sections covers the entire region in cross section/ LSP space that is anticipated from different types of Beyond the Standard Model theories in the above reference. This possibly suggests that we cannot use direct detection experiments to distinguish between *e.g.* SUSY versus Little Higgs versus Universal Extra Dimensions dark matter candidates in the absence of other data.

In Figure 13, we compare the WIMP-proton and WIMP-neutron cross sections in the spin-dependent and spin-independent cases. The spin-independent cross sections are seen to be fairly isospin independent; this is not the case, however, for the spin-dependent cross sections.

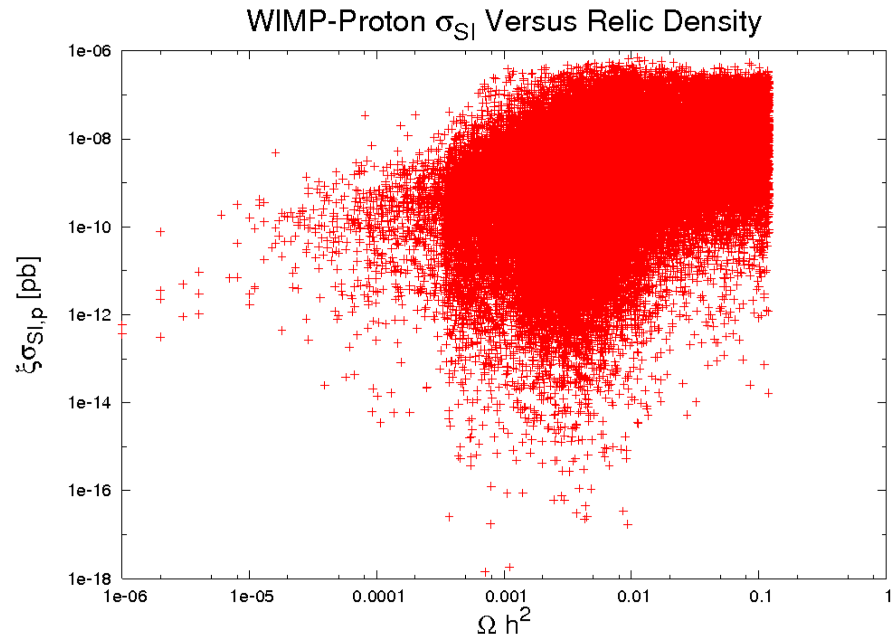

Figure 11. Distribution of scaled WIMP-proton spin-independent cross section versus the LSP contribution to relic density for our models.

3.4. Indirect Detection of Dark Matter

The PAMELA collaboration has recently claimed an excess in the ratio of cosmic ray positrons to electrons observed at energies $\gtrsim$ 10 GeV[49]. Here we employ DarkSUSY 5.0.4[50] to calculate this ratio for our model sample and compare these results with the PAMELA data.

In general, for a thermal relic dark matter candidate to reproduce the PAMELA data, its signal rate must be multiplied by a boost factor[51]. In nature, such a boost factor could result from, *e.g.*, a local overdensity. The boost factor in that case would be the square of the ratio between the density of dark matter in the region from which one is sensitive to cosmic ray positrons and electrons to the universe as a whole.

We have investigated four of the propagation models available as default choices in DarkSUSY: the model of Baltz and Edsjö(BE)[52], that of Kamionkowski and Turner(KT)[53], that of Moskalenko and Strong(MS)[54], as well as GALPROP[55]. In the figures that follow we show the results of calculations using the MS propagation model, which is based on early GALPROP Green's functions and whose results typically lie between those computed otherwise. However, we note that the extent to which the positron/electron flux ratio predicted by our models matches the PAMELA data can be highly sensitive to the choice of propagation model parameters and assumed astrophysical backgrounds. We will explore this further in future work[56]. The halo model employed here is the Navarro-Frenck-White profile[57].

The differential positron flux as a function of energy for a random sample of 500

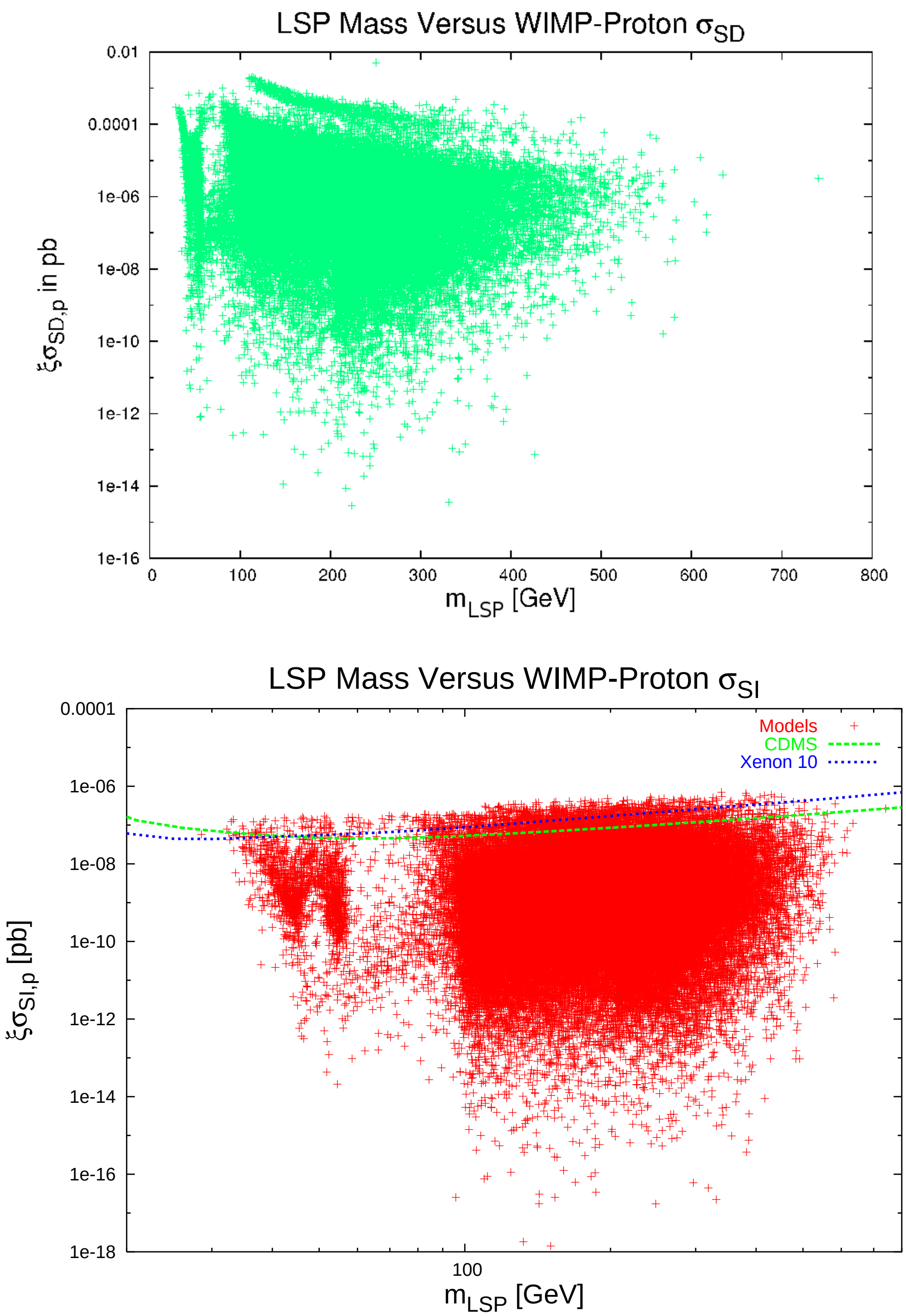

Figure 12. Distributions of scaled WIMP-proton spin-dependent cross section and spin-independent cross sections versus LSP mass in our models. In the spin-independent panel, the CDMS and Xenon10 bounds, which provide the strongest limits for the range in LSP mass relevant for our models, are shown.

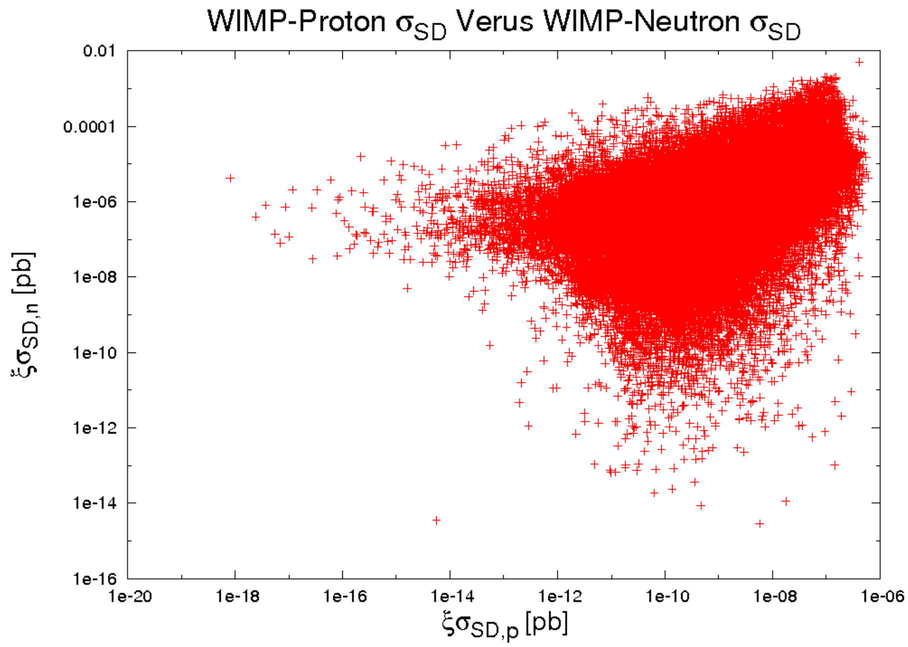

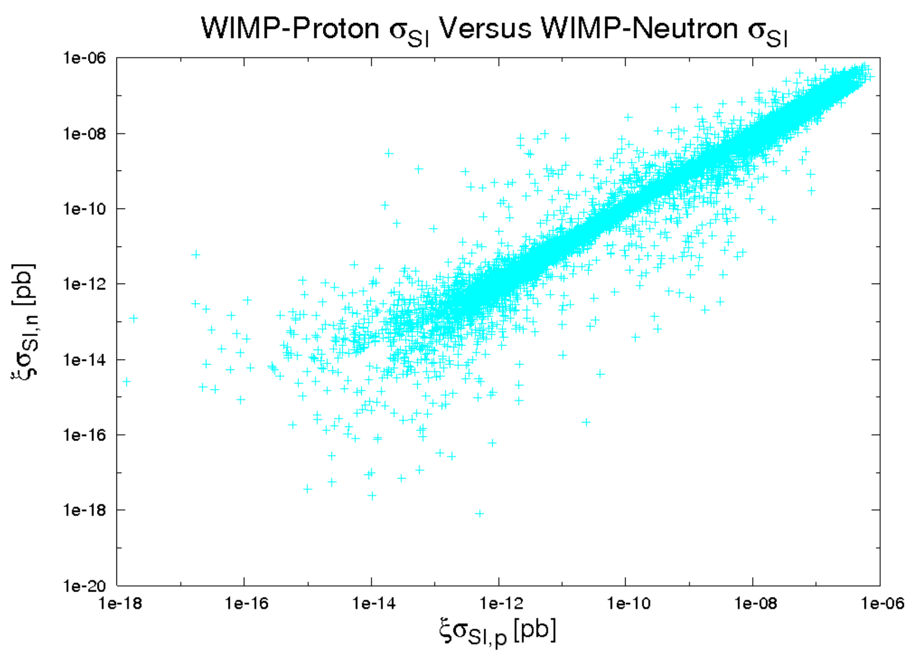

Figure 13. Here we compare WIMP-neutron and WIMP-proton cross sections. The spin-dependent cross sections are shown in the top panel; the spin-independent cross sections in the bottom panel.

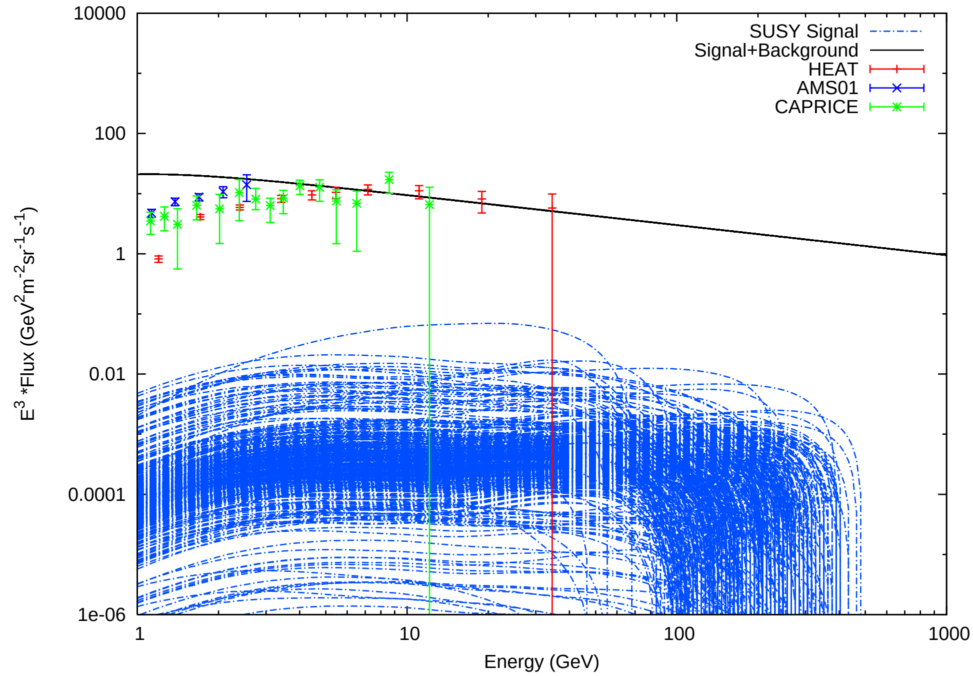

Figure 14. Expected, E^3 scaled, contribution to the absolute flux of positrons (unboosted) from neutralino annihilation in the halo for 500 randomly selected models employing MS propagation. Also shown are data from HEAT[61], AMS01[62], and CAPRICE94[63] as well as the DarkSUSY default secondary positron background (a parameterization of model 08-005 in[60].

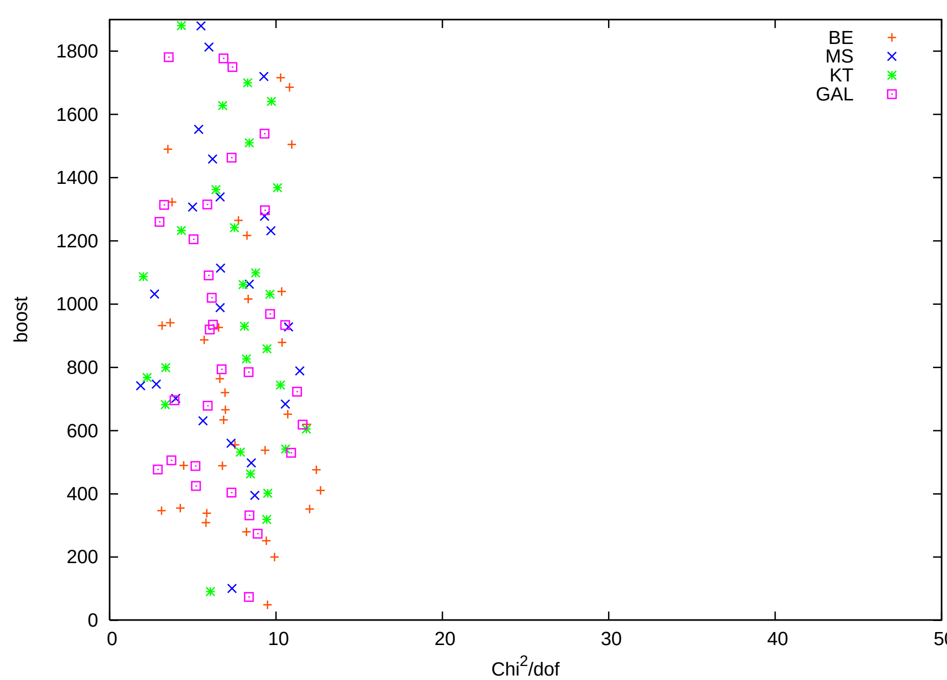

Figure 15. The distribution of χ^2 per degree of freedom versus the choice of boost factor that minimized this quantity for 500 randomly selected pMSSM models in our model set for the four propagation models discussed in the text.

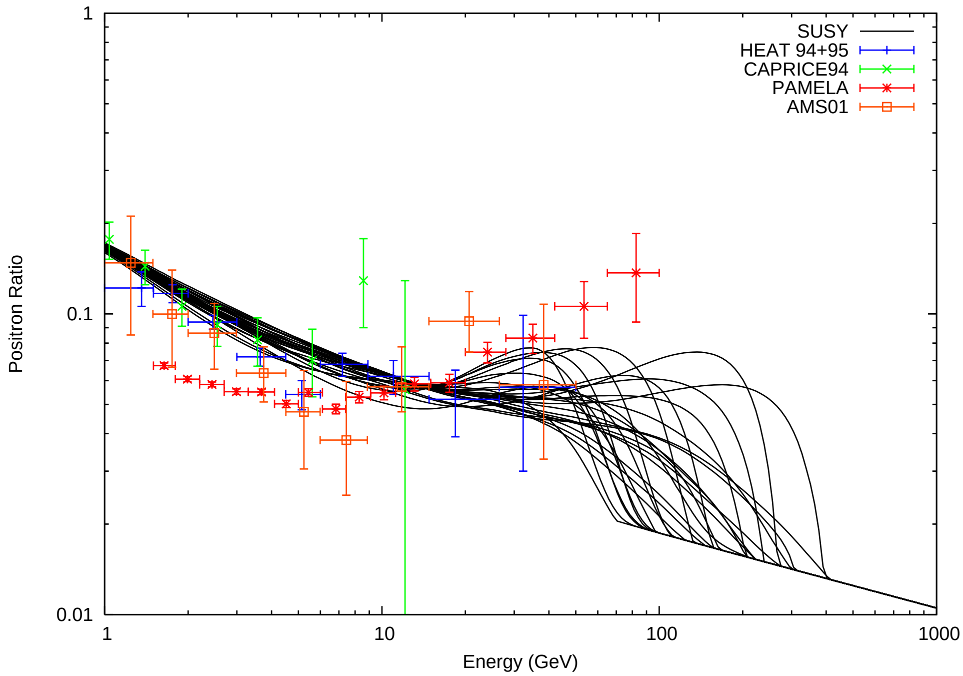

Figure 16. Positron/ electron flux ratio versus energy taking models from a set of 500 random pMSSM models for which the χ^2 per degree of freedom with the χ^2-maximizing boost was less than 10.0 for three of the four propagation models studied (curves shown use MS propagation). Data shown are from HEAT[64], CAPRICE94[63], PAMELA[49] and AMS01[62].

models from our set are shown in Figure 14. Here we assume a boost factor of 1; the normalization of the curves takes into account the fact that for many of these models $\Omega h^2|_{\rm LSP} < \Omega_{\rm WMAP}$.

We next determine how well the predicted positron fluxes for these models agree with the PAMELA data, allowing for the possibility of a boost factor. To do this, we find the value for the boost factor (with the restriction that it be < 2000) which minimizes the χ^2 for the fit of each model's prediction to the PAMELA data. (Note that many of the models require an even larger boost to obtain a good fit and are thus not shown in Figure 15). In calculating the χ^2, we consider only the seven highest energy bins, as at lower energies solar modulation is expected to play a major role[49]. Figure 15 shows the χ^2 and corresponding boost factor for these 500 random models. Note that there are four data points for each model in this figure. We then display the positron to electron flux ratio, for the models with a low value of χ^2 employing MS propagation, as a function of energy in Figure 16, and note the reasonable agreement with the data for some models.

Since the flux from WIMP annihilation scales as $(\Omega h^2|_{\rm LSP}/\Omega h^2|_{\rm WMAP})^2$, we might expect to improve the match to the PAMELA data using models from our sample for which $\Omega h^2|_{\rm LSP} \approx \Omega h^2|_{\rm WMAP}$. To test this, we examine the predicted positron flux for 500 random models with $\Omega h^2|_{\rm LSP} > 0.100$ employing MS propagation; these fluxes are

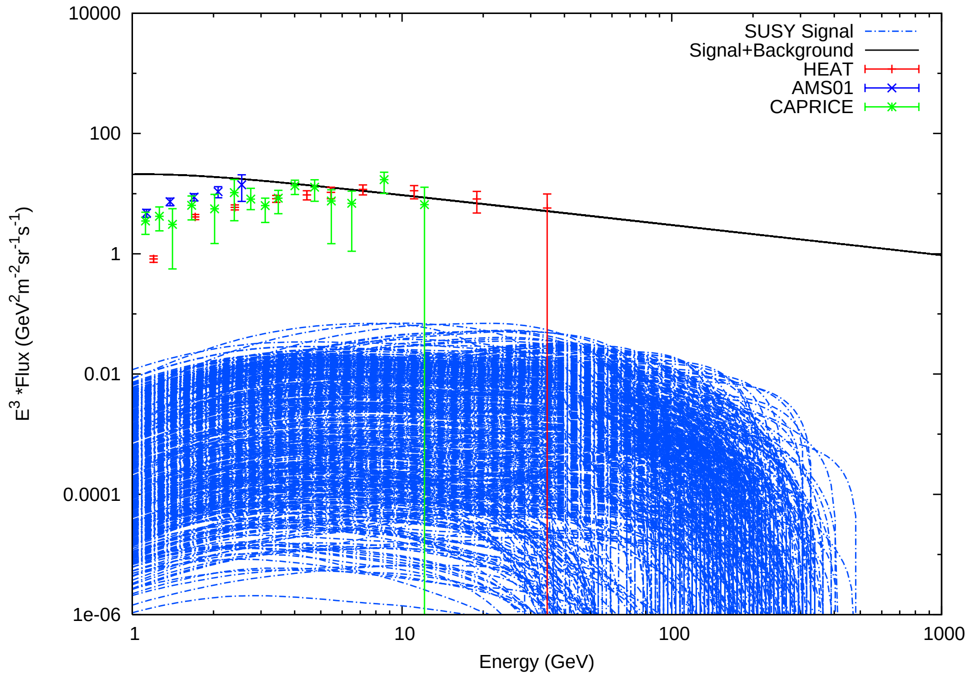

Figure 17. Same as Fig. 14 but now for a 500 model set satisfying $\Omega h^2|_{\mathrm{WMAP}} \geq \Omega h^2|_{\mathrm{LSP}} > 0.10$.

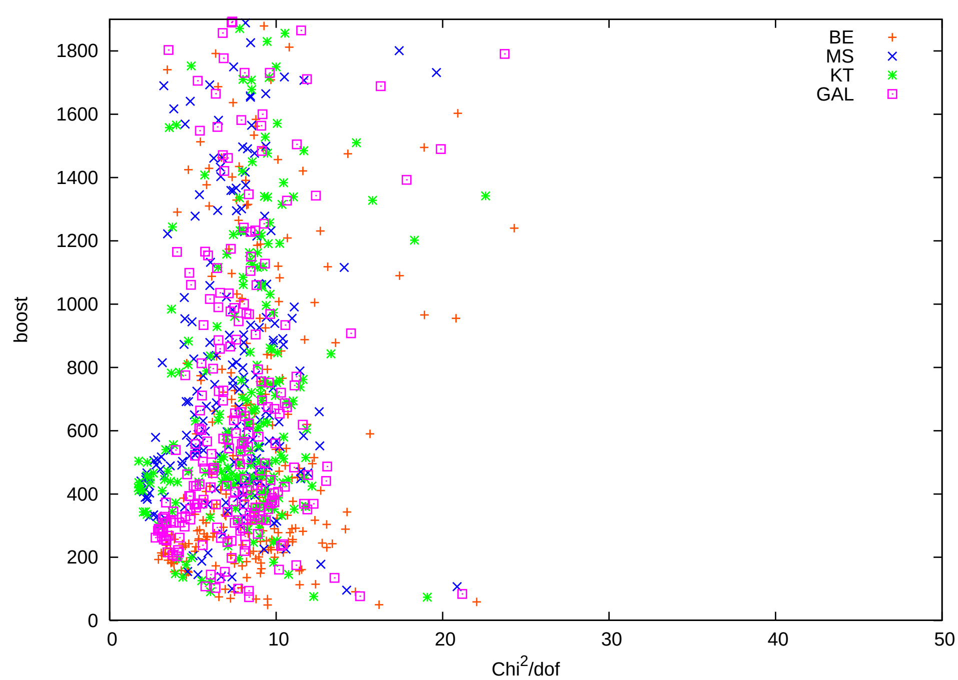

Figure 18. Same as Fig. 15 but now for a 500 model set satisfying $\Omega h^2|_{\mathrm{WMAP}} \geq \Omega h^2|_{\mathrm{LSP}} > 0.10$.

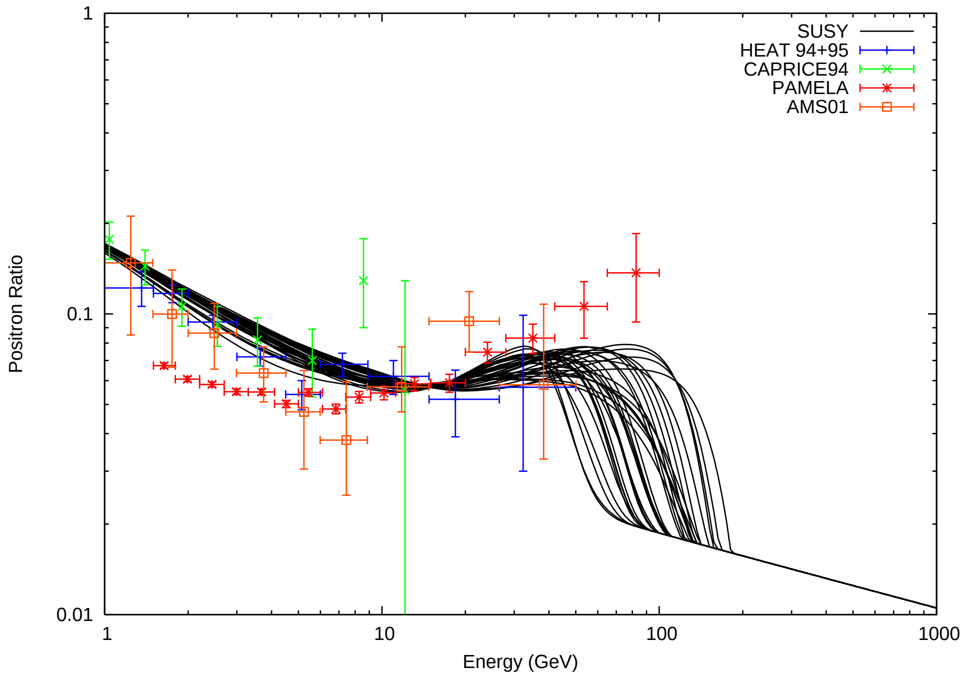

Figure 19. Positron/ electron flux ratio versus energy taking models from a set of 500 pMSSM models satisfying $\Omega h^2|_{\rm WMAP} \geq \Omega h^2|_{\rm LSP} > 0.10$ and for which χ^2-maximizing boost was less than 5.0 for three of the four propagation models studied (curves shown use MS propagation). Data shown are from HEAT[64], CAPRICE94[63], PAMELA[49] and AMS01[62].

shown in Figure 17 with no boost factor. We then again find the boost factor that minimizes the χ^2 of the positron to electron flux ratios with respect to the seven highest energy PAMELA bins; these are shown in Figure 18. Here, we note that there are many more models for which the χ^2-minimizing value for the boost factor is < 2000 and there are many more points for which the χ^2 value is low. The positron to electron flux ratios for these models, including the boost factor, are shown in Figure 19.

It appears that some of our models do a reasonably good job of fitting the PAMELA positron data, especially in the case where $\Omega h^2|_{\rm LSP}$ lies fairly close to the WMAP value. For most models, describing the PAMELA data requires large boost factors, however this is also a fairly generic feature of attempts to explain PAMELA and ATIC data in terms of WIMP annihilation[51]. There are however, many models which give relatively low χ^2 per degree of freedom in the fit to the data with relatively small boost factors. We will study this further in future work [56]. A study of the corresponding predictions for the the cosmic ray anti-proton flux is also underway.

4. Conclusions

We have generated a large set of points in parameter space (which we call "models") for the 19-parameter CP-conserving pMSSM, where MFV has been assumed. We subjected

these models to numerous experimental and theoretical constraints to obtain a set of ~ 68 K models which are consistent with existing data. We attempted to be somewhat conservative in our implementation of these constraints; in particular we only demanded that the relic density of the LSP not be greater than the measured value of Ωh^2 for non-baryonic dark matter, rather than assuming that the LSP must account for the *entire* observed relic density.

Examining the properties of the neutralinos in these models, we find that many are relatively pure gauge eigenstates with Higgsinos being the most common, followed by Winos. The relative prevalence of Higgsino and Wino LSPs leads many of our models to have a chargino as nLSP, often with a relatively small mass splitting between this nLSP and the LSP; this has important consequences in both collider and astroparticle phenomenology.

We find that, in general, the LSP in our models provides a relatively small ($\sim 4\%$) contribution to the dark matter, however there is a long tail to this distribution and a substantial number of models for which the LSP makes up all or most of the dark matter. Typically these neutralinos are mostly Binos.

Examining the signatures of our models in direct and indirect dark matter detection experiments, we find a wide range of signatures for both cases. In particular, we find, not unexpectedly a much larger range of WIMP-nucleon cross sections than is found in any particular model of SUSY-breaking as can be seen by comparing directly with the work in Ref.[48]. In fact, as these cross sections also enter the regions of parameter space suggested by non-SUSY models, it appears that the discovery of WIMPs in direct detection experiments might not be sufficient to determine the correct model of the underlying physics. As a first look at the signatures of these models in indirect detection experiments, we examined whether our models could explain the PAMELA excess in the positron to electron ratio at high energies. We find that there are models which fit the PAMELA data rather well where the LSP is mostly Bino, and some of these have significantly smaller boost factors than generally assumed for a thermal relic.

The study of the pMSSM presents exciting new possibilities for SUSY phenomenology. The next few years will hopefully see important discoveries both in colliders and in satellite or ground-based astrophysical experiments. It is important that we follow the data and not our existing prejudices; hopefully this sort of relatively model-independent approach to collider and astrophysical phenomenology can be useful in this regard.

Acknowledgments

The authors would like to thank C. F. Berger for her contributions during an earlier stage of this work. They would also like to thank J. Conley and D. Maitre for computational aid, T. Tait for discussions related to this work, and J. Baglio for his input during the initial stages of this analysis. RCC is supported by an NSF Graduate Research Fellowship. Work supported in part by the Department of Energy, Contract DE-AC02-

76SF00515.

References

[1] A. H. Chamseddine, R. L. Arnowitt and P. Nath, Phys. Rev. Lett. **49**, 970 (1982); E. Cremmer, P. Fayet and L. Girardello, Phys. Lett. B **122**, 41 (1983).

[2] G. F. Giudice and R. Rattazzi, Phys. Rept. **322**, 419 (1999) [arXiv:hep-ph/9801271]; M. Dine, A. E. Nelson, Y. Nir and Y. Shirman, Phys. Rev. D **53**, 2658 (1996) [arXiv:hep-ph/9507378].

[3] L. Randall and R. Sundrum, Nucl. Phys. B **557**, 79 (1999) [arXiv:hep-th/9810155]; G. F. Giudice, M. A. Luty, H. Murayama and R. Rattazzi, JHEP **9812**, 027 (1998) [arXiv:hep-ph/9810442].

[4] Z. Chacko, M. A. Luty, A. E. Nelson and E. Ponton, JHEP **0001**, 003 (2000) [arXiv:hep-ph/9911323]; D. E. Kaplan, G. D. Kribs and M. Schmaltz, Phys. Rev. D **62**, 035010 (2000) [arXiv:hep-ph/9911293].

[5] H. E. Haber and G. L. Kane, Phys. Rept. **117**, 75 (1985); S. P. Martin, arXiv:hep-ph/9709356; L. Pape and D. Treille, Rept. Prog. Phys. **69**, 2843 (2006); H.K. Dreiner, H.E. Haber, S.P. Martin, "Two-component spinor techniques and Feynman rules for quantum field theory and supersymmetry," SCIPP-08/08, submitted to **Phys. Rep.**; M. Drees, R. Godbole and P. Roy, *Hackensack, USA: World Scientific (2004) 555 p*; H. Baer and X. Tata, *Cambridge, UK: Univ. Pr. (2006) 537 p.* S. Dimopoulos and D. Sutter, Nucl. Phys. B452, 496 (1995); D.W. Sutter, Stanford Ph. D. thesis, hep-ph/9704390. D. J. H. Chung, L. L. Everett, G. L. Kane, S. F. King, J. D. Lykken and L. T. Wang, "The soft supersymmetry-breaking Lagrangian: Theory and applications," Phys. Rept. **407**, 1 (2005) [arXiv:hep-ph/0312378].

[6] For a review, see, G. D'Ambrosio, G. F. Giudice, G. Isidori and A. Strumia, Nucl. Phys. B **645**, 155 (2002) [arXiv:hep-ph/0207036].

[7] A. Djouadi, J. L. Kneur and G. Moultaka, Comput. Phys. Commun. **176**, 426 (2007) [arXiv:hep-ph/0211331].

[8] C. F. Berger, J. S. Gainer, J. L. Hewett and T. G. Rizzo, JHEP **0902**, 023 (2009) [arXiv:0812.0980 [hep-ph]].

[9] G. Belanger, F. Boudjema, A. Pukhov and A. Semenov, Comput. Phys. Commun. **177** (2007) 894; arXiv:0803.2360 [hep-ph]; Comput. Phys. Commun. **149**, 103 (2002) [arXiv:hep-ph/0112278]; Comput. Phys. Commun. **174**, 577 (2006) [arXiv:hep-ph/0405253]; Comput. Phys. Commun. **176**, 367 (2007) [arXiv:hep-ph/0607059] and arXiv:0803.2360 [hep-ph].

[10] G. Isidori and P. Paradisi, Phys. Lett. B **639**, 499 (2006) [arXiv:hep-ph/0605012].

[11] D. Eriksson, F. Mahmoudi and O. Stal, arXiv:0808.3551 [hep-ph].

[12] G. W. Bennett *et al.* [Muon G-2 Collaboration], Phys. Rev. D **73**, 072003 (2006) [arXiv:hep-ex/0602035].

[13] For an introduction, see, J. S. Hagelin, S. Kelley and T. Tanaka, Nucl. Phys. B **415**, 293 (1994); F. Gabbiani, E. Gabrielli, A. Masiero and L. Silvestrini, Nucl. Phys. B **477**, 321 (1996) [arXiv:hep-ph/9604387].

[14] C. Amsler *et al.* [Particle Data Group], Phys. Lett. B **667**, 1 (2008).

[15] Heavy Flavor Averaging Group, http://www.slac.stanford.edu/xorg/hfag/.

[16] M. Misiak *et al.*, Phys. Rev. Lett. **98**, 022002 (2007) [arXiv:hep-ph/0609232].

[17] T. Becher and M. Neubert, Phys. Rev. Lett. **98**, 022003 (2007) [arXiv:hep-ph/0610067].

[18] The preliminary combined CDF and D0 limit was presented by D. Toback, talk given at Physics for LHC-2008, Split, Croatia, 29 Sept.-4 Oct. 2008. See also T. Aaltonen *et al.* [CDF Collaboration], Phys. Rev. Lett. **100**, 101802 (2008) [arXiv:0712.1708 [hep-ex]].

[19] M. Passera, W. J. Marciano and A. Sirlin, arXiv:0809.4062 [hep-ph].

[20] E. De Rafael, arXiv:0809.3085 [hep-ph].

[21] P. Chang, K. Hara and T. Hurth, talks given at the 34th International Conference on High Energy Physics, Philadelphia, PA, 29 July-5 Aug, 2008.

[22] G. Benelli, "Search for stable and long lived heavy charged particles in electron positron collisions at center of mass energies from 130-GeV to 209-GeV with the OPAL detector at LEP," UMI-31-09638, 2003. 126pp.

[23] LEP Electroweak Working Group, http://www.cern.ch/LEPEWWG.
[24] R. Barate *et al.* [ALEPH Collaboration], Phys. Lett. B **469**, 303 (1999).
[25] A. C. Kraan, arXiv:hep-ex/0305051.
[26] LEP SUSY Working Group, http://lepsusy.web.cern.ch/lepsusy/.
[27] LEP Higgs Working Group, http://lephiggs.web.cern.ch/LEPHIGGS/www/Welcome.html.
[28] A. Djouadi, M. M. Muhlleitner and M. Spira, Acta Phys. Polon. B **38**, 635 (2007) [arXiv:hep-ph/0609292]; http://lappweb.in2p3.fr/~tmuehlleitner/SUSY-HIT/.
[29] For a review, see, for example, S. Heinemeyer, W. Hollik and G. Weiglein, Phys. Rept. **425**, 265 (2006) [arXiv:hep-ph/0412214].
[30] V. M. Abazov *et al.* [D0 Collaboration], Phys. Lett. B **660**, 449 (2008) [arXiv:0712.3805 [hep-ex]].
[31] T. Sjostrand, S. Mrenna and P. Skands, JHEP **0605**, 026 (2006) [arXiv:hep-ph/0603175].
[32] J. Conway, PGS4, Pretty Good detector Simulation, http://www.physics.ucdavis.edu/~conway/research/software/pgs/pgs.html.
[33] W. Beenakker, R. Hopker and M. Spira, arXiv:hep-ph/9611232. See also, http://www.ph.ed.ac.uk/~tplehn/prospino/. The NLO squark and gluino cross section are given in W. Beenakker, R. Hopker, M. Spira and P. M. Zerwas, Nucl. Phys. B **492**, 51 (1997) [arXiv:hep-ph/9610490].
[34] G. J. Feldman and R. D. Cousins, Phys. Rev. D **57**, 3873 (1998) [arXiv:physics/9711021].
[35] T. Aaltonen *et al.* [CDF Collaboration], arXiv:0808.2446 [hep-ex].
[36] A. Duperrin [CDF Collaboration and D0 Collaboration], arXiv:0710.4265 [hep-ex]. For a recent update, see S. Lowette, talk given at the 34th International Conference on High Energy Physics, Philadelphia, PA, 29 July-5 Aug, 2008. For the latest overview, see Tevatron New Phenomena and Higgs Working Group, http://tevnphwg.fnal.gov/.
[37] V. M. Abazov *et al.* [D0 Collaboration], arXiv:0809.4472 [hep-ex].
[38] T. Aaltonen *et al.* [CDF Collaboration], Phys. Rev. Lett. **101**, 071802 (2008) [arXiv:0802.3887 [hep-ex]]; CDF Note CDF/PUB/TOP/PUBLIC/9343; D0 Note 5598-CONF; CDF Note 9332; V. M. Abazov *et al.* [D0 Collaboration], Phys. Rev. Lett. **97**, 171806 (2006) [arXiv:hep-ex/0608013]; V. Buescher *et al.* [CDF and DO Collaborations], arXiv:hep-ex/0504004; V. M. Abazov *et al.* [D0 Collaboration], Phys. Lett. B **665**, 1 (2008) [arXiv:0803.2263 [hep-ex]]; T. Aaltonen *et al.* [CDF Collaboration], Phys. Rev. D **76**, 072010 (2007) [arXiv:0707.2567 [hep-ex]].
[39] E. Komatsu *et al.* [WMAP Collaboration], arXiv:0803.0547 [astro-ph].
[40] For recent overviews see G. Gelmini, talk given at the 34th International Conference on High Energy Physics, Philadelphia, PA, 29 July-5 Aug, 2008 and U. Oberlack, talk given at COSMO '08, Madison, WI, Aug. 2008; G. Gerbier, talk given at SUSY 008, Seoul, Korea, June 2008. See also J. D. Vergados, Lect. Notes Phys. **720**, 69 (2007) [arXiv:hep-ph/0601064].
[41] U. Oberlack [XENON Collaboration], J. Phys. Conf. Ser. **110**, 062020 (2008).
[42] Z. Ahmed *et al.* [CDMS Collaboration], arXiv:0802.3530 [astro-ph].
[43] M. Bravin *et al.* [CRESST-Collaboration], Astropart. Phys. **12**, 107 (1999) [arXiv:hep-ex/9904005].
[44] R. Bernabei *et al.* [DAMA Collaboration], Phys. Lett. B **480**, 23 (2000).
[45] J. A. Conley, J. S. Gainer, J. L. Hewett, and T. G. Rizzo. In preparation.
[46] N. Arkani-Hamed and S. Dimopoulos, JHEP **0506**, 073 (2005) [arXiv:hep-th/0405159]; G. F. Giudice and A. Romanino, Nucl. Phys. B **699**, 65 (2004) [Erratum-ibid. B **706**, 65 (2005)] [arXiv:hep-ph/0406088].
[47] There have been many such a analyses; a few recent representative examples are: B. C. Allanach, M. J. Dolan and A. M. Weber, JHEP **0808**, 105 (2008) [arXiv:0806.1184 [hep-ph]]; S. S. AbdusSalam, arXiv:0809.0284 [hep-ph]; O. Buchmueller *et al.*, arXiv:0808.4128 [hep-ph]; R. Trotta, F. Feroz, M. P. Hobson, L. Roszkowski and R. R. de Austri, arXiv:0809.3792 [hep-ph]; L. Roszkowski, R. Ruiz de Austri and R. Trotta, JHEP **0707**, 075 (2007) [arXiv:0705.2012 [hep-ph]], JHEP **0704**, 084 (2007) [arXiv:hep-ph/0611173] and JHEP **0605**, 002 (2006) [arXiv:hep-ph/0602028]; U. Chattopadhyay and D. Das, arXiv:0809.4065 [hep-

ph]; S. Heinemeyer, X. Miao, S. Su and G. Weiglein, arXiv:0805.2359 [hep-ph]; J. R. Ellis, S. Heinemeyer, K. A. Olive, A. M. Weber and G. Weiglein, JHEP **0708**, 083 (2007) [arXiv:0706.0652 [hep-ph]]; E. A. Baltz, M. Battaglia, M. E. Peskin and T. Wizansky, Phys. Rev. D **74**, 103521 (2006) [arXiv:hep-ph/0602187]; J. Ellis, S. F. King and J. P. Roberts, JHEP **0804**, 099 (2008) [arXiv:0711.2741 [hep-ph]].

[48] V. Barger, W. Y. Keung and G. Shaughnessy, arXiv:0806.1962 [hep-ph].

[49] O. Adriani *et al.*, arXiv:0810.4995 [astro-ph].

[50] P. Gondolo, J. Edsjö, P. Ullio, L. Bergstrom, M. Schelke and E. A. Baltz, JCAP **0407**, 008 (2004) [arXiv:astro-ph/0406204]. P. Gondolo, J. Edsj, P. Ullio, L. Bergstrm, M. Schelke, E.A. Baltz, T. Bringmann and G. Duda, http://www.physto.se/~edsjo/darksusy.

[51] This is a fairly generic result, see for example: M. Cirelli, M. Kadastik, M. Raidal and A. Strumia, arXiv:0809.2409 [hep-ph]. I. Cholis, L. Goodenough, D. Hooper, M. Simet and N. Weiner, arXiv:0809.1683 [hep-ph]. D. Hooper and K. Zurek, arXiv:0902.0593 [hep-ph].

[52] E. A. Baltz and J. Edsjö, Phys. Rev. D **59**, 023511 (1999) [arXiv:astro-ph/9808243].

[53] M. Kamionkowski and M. S. Turner, Phys. Rev. D **43**, 1774 (1991). M. S. Turner and F. Wilczek, Phys. Rev. D **42**, 1001 (1990).

[54] I. V. Moskalenko and A. W. Strong, Phys. Rev. D **60**, 063003 (1999) [arXiv:astro-ph/9905283].

[55] http://galprop.stanford.edu/web_galprop/galprop_home.html.

[56] R. C. Cotta, J. S. Gainer, J. L. Hewett, and T. G. Rizzo. In preparation.

[57]

[58] J. F. Navarro, C. S. Frenk and S. D. M. White, Astrophys. J. **490**, 493 (1997) [arXiv:astro-ph/9611107].

[59] J. F. Navarro, C. S. Frenk and S. D. M. White, Astrophys. J. **462**, 563 (1996) [arXiv:astro-ph/9508025].

[60] I. V. Moskalenko and A. W. Strong, Astrophys. J. **493**, 694 (1998) [arXiv:astro-ph/9710124].

[61] M. A. DuVernois *et al.* [HEAT Collaboration], Astrophys. J. **559**, 296 (2001).

[62] M. Aguilar *et al.* [AMS Collaboration], Phys. Rept. **366**, 331 (2002) [Erratum-ibid. **380**, 97 (2003)].

[63] Boezio, M. *et al.* [CAPRICE Collaboration],

[64] S. W. Barwick *et al.* [HEAT Collaboration], Astrophys. J. **482**, L191 (1997) [arXiv:astro-ph/9703192].